J. Eng. Technol. Sci., Vol. 53, No. 2, 2021, 210201

Toward Improvement of Resistance Testing Reliability

I Ketut Aria Pria Utama[1*], Dian Purnamasari[2], I Ketut Suastika[1], Nurhadi[2] & Giles Anthony Thomas[3]

[1]Department of Naval Architecture, Sepuluh Nopember Institute of Technology (ITS), Keputih, Sukolilo, Surabaya 60111, Indonesia
[2]IHL, Agency for The Assessment and Application of Technology (BPPT), Jalan Hidrodinamika BPPT, Kompleks ITS Sukolilo, Surabaya 60112, Indonesia
[3]Department of Mechanical Engineering, University College London, Gower Street, London, United Kingdom
*E-mail: kutama@na.its.ac.id

Highlights:

- The accuracy of resistance predictions was evaluated by implementing the ISO GUM in the tests to identify all significant sources of uncertainty.
- Potential influences on the resistance results were identified by filtering the raw signal, water temperature and calibration.
- To obtain approximations of the true values of resistance measurement, the Kalman filter gains were tuned using an evolutionary algorithm to minimize the standard deviation from the sample resistance data.
- Reliable results can be obtained by optimization of the standard deviation with the application of a Kalman filter.

Abstract. Periodically conducting a benchmark test with estimated uncertainty is important to improve the quality of resistance predictions and understand the influence of instrumentation, testing procedures and analysis techniques. The LHI-007 Ro-Ro Ferry ship model, made available by the Maritime Research Institute Netherlands (MARIN), was used for benchmark testing from 2010 to 2018 at the Indonesian Hydrodynamic Laboratory. Comparisons were made between filtering the resistance data with a low-pass filter and with a Kalman filter. This work shows how benchmark tests can be used to track test performance over a longer period and proposes techniques to improve the uncertainty in the resistance results.

Keywords: *benchmark test; Kalman filter; low-pass filter; resistance; uncertainty analysis.*

1 Introduction

Experimental fluid dynamics (EFD) research in a towing tank is often conducted in the design stage to understand the physics of a ship's hydrodynamic performance. In particular the magnitude of ship resistance is important for ship designers when specifying ship power requirements [1]. The most typical towing tank tests measure the resistance when a ship model is towed by a carriage and

Received June 11TH, 2019, 1st Revision March 17th, 2020, 2nd Revision March 26th, 2020, 3rd Revision July 21st, 2020, 4th Revision August 8th, 2020, Accepted for publication November 19th, 2020.
 ISSN: 2337-5779,
DOI: 10.5614/j.eng.technol.sci.2021.53.2.1

the total longitudinal force acting on the model is measured for various speeds. Due to the requirement of high-quality experimental results, the accuracy of the measurements and the robustness of the tank tests need to be verified. This can be achieved by comparison with previous results and by implementing the *ISO Guide to the Expression of Uncertainty in Measurement* (ISO GUM) in the resistance tests to identify all significant sources of uncertainty [2].

Benchmark tests ensure that the equipment, test procedures and analysis techniques are adequate. Benchmark testing at the Indonesian Hydrodynamic Laboratory (IHL) was commenced in 2010 and repeated annually until 2018. The LHI-007 Ro-Ro Ferry ship model was chosen as the target model because it was originally used as a benchmark in 1994, when the facility was commissioned with identical tests conducted at both the Maritime Research Institute Netherlands (MARIN) and IHL [3]. As in most experiments, the mean value of the measured signal was used as the key output of the resistance measurement and analysis. It is also important to identify the magnitude of the uncertainty of the resistance test results. In order to improve the measurement quality, the contributions of various factors or noise sources need to be identified. In the preliminary phase, the autocovariance method is used for variance analysis on stationary measurements to compare the quality of quasi-steady measurement methods, as discussed in [4]. Brouwer, *et al.* [5] proposed the novel Transient Scanning Technique for verifying the stationarity of the signal and conducting an uncertainty analysis of a finite-length measurement time series. Steen, *et al.* [6] analyzed resistance data in multiple (instead of single) time windows and carried out a comparison of simulated and measured towing force. This allowed them to conclude that the noise in the carriage speed was the main contributor to noise in the resistance data and thus the uncertainty of the mean value could be reduced. Recently, a new power spectrum based method has been developed to determine the spectral contribution to the uncertainty of the mean, which was applied to the resistance data of a ship model [7].

The availability of CFD has been recognized to be important for resistance prediction. Comparison between computed results and measured data is done to evaluate the accuracy of CFD simulations. The simulation and experimental results of the flow field around a fast ship has shown that computation of medium Froude numbers $Fr < 0.25$ is an efficient and accurate tool to predict the curves of resistance for ship flow [8]. Investigation of the resistance components for converting a traditional mono-hull fishing vessel into a catamaran and the results of CFD were in good agreement with well-known empirical formulas used by commercial design software (Maxsurf) and slender body theory with an order of magnitude error less than 5% [9]. Suastika, *et al.* [10] investigated the influence of the parallel-middle-body relative length and stern form on the formation of wake behind single-screw large ships and found that an increase in the parallel-middle-body relative length for ships with the same stern form resulted in an increase in the drag coefficient.

The objective of this work was to increase the accuracy of resistance predictions by implementing the ISO GUM procedure in tests to identify significant sources of uncertainty. Then, the influence of two potential filters on the resistance results was investigated with a Kalman filter developed in MATLAB^{TM} and a lowpass filter from Sigview signal analysis tools [11] for offline execution. The work builds on previous studies into benchmarks and uncertainty analysis for ship-model resistance tests [12-14].

2 Method

2.1 Model Geometry

The LHI-007 Ro-Ro Ferry ship model was selected as the target of the benchmark tests; the scale ratio of the model was 1:20.97. The main particulars of the ship and the model are presented in Table 1. The Ro-Ro Ferry model is shown in Figure 1. The resistance tests were executed in free-model conditions at Froude number varying from *Fr* = 0.15 to *Fr* = 0.29.

Table 1 Principal particulars of ship and model.

Model characteristics	Symbol	Ship	Model	Unit
Length on waterline	*Lwl*	146.94	7.007	m
Breadth	B	24.00	1.150	m
Draft	*T*	6.50	0.310	m
Wetted surface area	*S*	4042.00	10.392	m^2
Displacement Volume	∇	14.21	1.579	m^3
Block coefficient	C_b	0.80	0.80	

Figure 1 The LHI-007 model.

An example of the raw resistance data (from tests conducted in 2012) is shown in Figure 2. The measurement of resistance for the range of speed from 1.24 to 2.48 m/s was obtained by averaging the time history of the signal from the data acquisition system for time interval $\Delta t = N/fs$, where Δt is time, N is the number of sampling data points, and *f*s is the sampling rate. Data acquisition was done through the collection of 1050 samples over 35 seconds at 30 Hz.

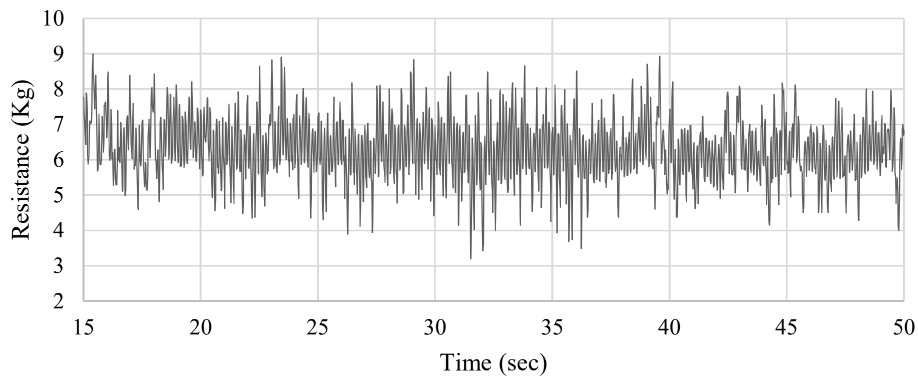

Figure 2 Sample time history of benchmark resistance data at speed 1.91 m/s and temperature 2.78 °C. The resistances measured was 6.24 kg (2012).

The tests were conducted at the Indonesian Hydrodynamics Laboratory towing tank facility, which is 234.5 m long (including the harbor model) and 11 m wide and has a water depth of 5.5 m. The model should be attached to the measuring head of the resistance dynamometer by a connection that can transmit and measure only the horizontal tow force; guides may be fitted to prevent the model from yawing or swaying.

The tow force should, if possible, be applied in the line of the propeller shaft and at the LCB in order to avoid artificial trim effects. The data acquisition may begin after a steady speed has been reached, as shown in Figure 3. Resistance was measured at nine forward speeds, corresponding to Froude numbers 0.15 to 0.29. The resistance values of the ship model were estimated for calm water conditions without appendages (rudder and propeller).

The procedure to estimate the standard deviation starts by estimating the applicable window width (influence width). The measured time series $x_i(t)$ with finite length T was considered as a stationary random process $\{x(t)\}$ [15] (see also

[16]). The sample time-average *mi* is an estimator of the mean of the process, as expressed in Eq. (1):

$$m_i = \frac{1}{T}\int_0^T x_i(t)\, dt \quad (1)$$

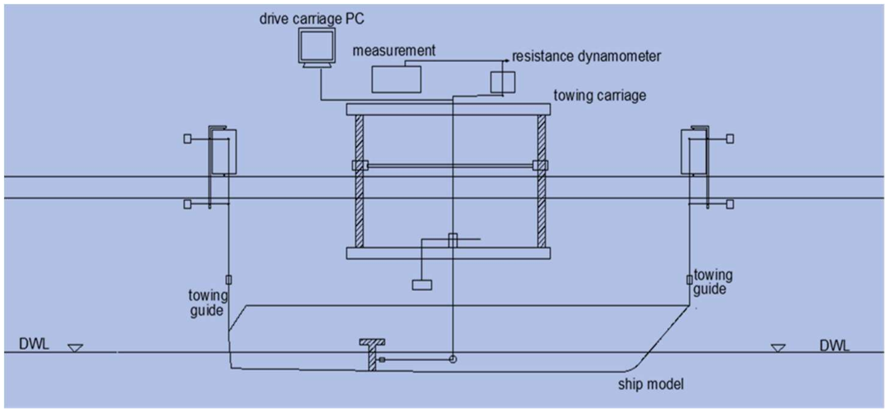

Figure 3 Experimental set-up.

The standard deviation of time history and the standard uncertainty respectively for single measurements can be obtained [17] (see also [18]), as expressed in Eq. (2):

$$s = \sqrt{\frac{1}{n-1}\sum_{i=1}^{n}(R_T - R_{Ti})} \quad (2)$$

where R_{Ti} is the *i*-th data point of the time series, R_T is the total resistance and n is the number of sampling data points.

The measured resistance was non-dimensionalized as the total resistance coefficient, C_T, using the following equation:

$$C_T = \frac{R_T}{(0.5\, \rho S V^2)} \quad (3)$$

2.2 Uncertainty Analysis for Resistance

Special consideration was given to the integration of the uncertainty assessments in all phases of the experimental process as recommended by the International Towing Tank Conference (ITTC) [19]. The relative standard uncertainty components of resistance related to the hull geometry can be estimated by Eq. (4):

$$u_1'(R_T) = u'(S) = \frac{2}{3}u'(\Delta) \tag{4}$$

where *u'(S)* is the uncertainty component of the wetted surface area of the ship model, Δ is the uncertainty component of the displacement volume of the ship model.

The uncertainty of resistance resulted from the towing speed is obtained quantitatively with the equation:

$$u_2'(R_T) = 2u'(V) \tag{5}$$

where *u'(V)* is the uncertainty of the towing speed.

The relative standard uncertainty of resistance is estimated with Eq. (6):

$$u_3'(R_T) = \frac{C_F}{C_T}\frac{0.87}{log_{10}\,Re-2}\,u'(\nu) \tag{6}$$

where C_F is the coefficient friction, C_T is the total resistance coefficient, *Re* is the Reynold's number, and *u'(ν)* is the uncertainty component of the water viscosity affected by temperature.

The uncertainty component of the resistance resulted from the calibration of the dynamometer is estimated by standard error estimation (*SEE*) using Eq. (7):

$$u_4'(R_T) = SEE \tag{7}$$

The standard uncertainty component from single test tests can be estimated with the following equation:

$$u_5'(R_T) = s \tag{8}$$

These are then combined to obtain the overall standard uncertainty by the root-sum-squares method as follows:

$$u_c' = \sqrt{(u_1')^2 + (u_2')^2 + (u_3')^2 + (u_4')^2 + (u_5')^2} \tag{9}$$

The expanded standard uncertainty of the resistance with confidence level (t) is estimated using Eq. (10):

$$U_P(R_T) = k_P.u_c'(R_T) \tag{10}$$

where k_p is the coverage factor.

2.3 **Resistance Results**

Resistance benchmark experiments were conducted between 2010 and 2018, with all resistance tests being conducted under the same conditions. Speeds were varied from 11 to 22 knots (full scale); the corresponding towing speeds at model scale were 1.24 to 2.92 m/s (Froude numbers from 0.15 to 0.29). The different data sets are shown in Figure 4. On the basis of the collected data, the experimental results appeared to agree well over the years.

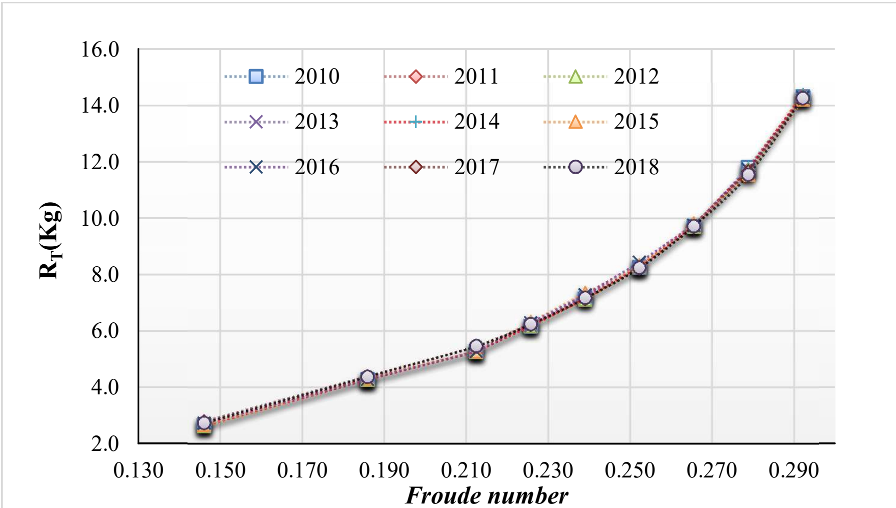

Figure 4 Total resistance model of LHI-007.

When some tests are repeated, all resistance measurements should also be corrected to the nominal speed that corresponds to the prescribed Froude number, as shown in Eq. (11):

$$Fr = \frac{V}{\sqrt{gL}} \tag{11}$$

The effect of temperature is included in the Reynold's number, as shown in Eq. (12).

$$Re = \frac{VL}{\nu} \tag{12}$$

The resistance results for each speed are shown in Figure 5 as a percentage deviation from the original 1994 test results. These results show that it was hardest to maintain low deviations for resistance values at low speed (Fr = 0.15 and 0.19). In contrast, the results for the speed range Fr = 0.21 to 0.29 were generally within 1% to 2% deviation, showing good repeatability over the years. The combination of the uncertainty components, as estimated relating to the total resistance measurement at Fr = 0.25 as operational speed, are summarized in Table 2.

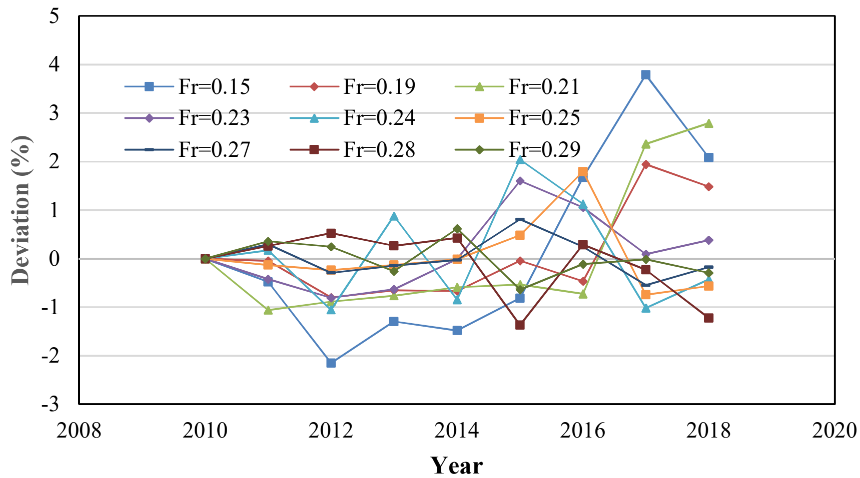

Figure 5 The deviations of the resistance results from those measured in 1994.

Table 2 Combined uncertainty (fr = 0.25) before filtering.

R_T (*Fr* = 0.25)	2010	2011	2012	2013	2014	2015	2016	2017	2018
Wetted area	0.126	0.126	0.126	0.126	0.126	0.126	0.126	0.126	0.126
Dynamometer	0.073	0.217	0.233	0.405	0.588	0.588	0.585	0.549	0.344
Temperature	0.175	0.179	0.166	0.166	0.173	0.166	0.166	0.175	0.166
Speed	0.066	0.066	0.066	0.066	0.066	0.066	0.066	0.066	0.066
Single test (deviation)	0.758	0.721	0.742	0.752	0.742	0.765	0.751	0.885	0.839
Combined	0.794	0.787	0.808	0.882	0.973	0.989	0.977	1.066	0.933

2.4 Potential Influences on Resistance Test Results

Potential influences on the resistance results were identified by filtering the raw signal, water temperature and calibration.

2.5 Filtering

Special consideration should be given to the time history of the data sampling. It is recommended that the sampling rate, time interval and cut-off frequency of low-pass filtering are properly chosen. The most appropriate low-pass cut-off frequency was about 1.0 to 3.0 Hz, using the Sigview software [20]. This was first determined by conducting an optimized fast Fourier transform (FFT) of the raw data to understand at what frequency there was noise in the signal.

2.6 Water Temperature

When the original data were determined at a specific water temperature but later tests were conducted at other temperatures, the temperature data are needed in order to determine the suitability of the temperature coefficient measurements. The density and viscosity of the water in the towing tank were calculated based on the water temperature according to the ITTC method [21]. Deviations in water temperature have a relatively large effect on water density and viscosity and thereafter on the model mass displacement (to keep the volume of displacement equivalent) as well as the Reynold's number and the frictional drag of the model.

2.7 Calibration

The dynamometer used for measuring the longitudinal force should be calibrated with weights. The weights provide the standard for the load cell calibration and thus are a potential source of error. The calibration of the resistance dynamometer should be carried out before the tests according to the ITTC method [22]. Calibration diagrams of measured quantities (output values) are plotted against the calibration units (input units); the calibration provides guidance on the linearity of the instrument response.

2.8 Analysis

For further analysis of the resistance measurements, the standard Kalman Filter (KF) was used on the raw resistance data. The iterations of the Kalman filter can be written as follows:

The time update of the predicted state estimate is obtained by:

$$\hat{x}_k^- = Az_{k-1} + \boldsymbol{F} \tag{13}$$

The prediction error covariance is obtained quantitatively by:

$$P_k^- = AH_{k-1}A^T + Q \tag{14}$$

The Kalman gain measurement update is obtained by:

$$K_k = P_k^- H^T (HP_k^- H^T + R)^{-1} \tag{15}$$

The estimation measurement update is obtained by:

$$\hat{x}_k = \hat{x}_k^- + K(z_k - H\hat{x}_k^-) \tag{16}$$

The update error covariance is obtained by:

$$P_k = (1 - K_k H)P_k^- \tag{17}$$

where:

$\hat{x}_k^-$ is the a priori state estimate, $\hat{x}_k$ is the a posteriori state estimate, A is the metric distance between the a priori state and the update state, and F is the metric distance between the input and the update state, P_k^- is the a priori covariance, P_k is the a posteriori covariance, H is the metric distance between the update state and the measurement, Q is the process noise covariance, R is the measurement noise covariance, and K is the Kalman gain.

In the treatment here, it was assumed that there were uncorrelated Gaussian stationary white-noise sequences with zero mean. Process noise covariance Q and measurement noise covariance R are important parameters to decide the prediction's closeness to the true value. To study the difference between the estimated value and the true value, the value of Q is changed while measurement noise covariance R is kept the same and, conversely, R is changed while keeping Q constant. This will have consequences for the Kalman gain regarding the result of the Kalman filter.

3 Results and Discussion

The predominant sources of uncertainty in the resistance measurements were investigated using the ITTC method. The standard uncertainty of resistance consists of several components, i.e. model geometry, instrument calibration, and direct measurement. The uncertainty of the model hull was determined by its displacement Δ, which can be determined by the displacement volume and the mass density of the towing tank water at the temperature during the tests. Herein, the same model was tested at different dates, with a change of several degrees in water temperature. The hull model was adjusted to the water temperature corresponding to the specific date. The influence of the uncertainty of the water density on the true displacement volume of the hull model in the tank water is shown in Table 3.

Table 3 Temperature Variation of Water in the Towing Tank

Year	Temperature (°C)	Density (kg/m^3)	Kinematic Viscosity (m^2/s)	Displacement (Δ) (kg)
1994	28	996.236	$8.35.10^{-7}$	153.562
2010	27	996.515	$8.54.10^{-7}$	153.557
2011	27.1	996.488	$8.52.10^{-7}$	153.527
2012	27.8	996.292	$8.39.10^{-7}$	153.505
2013	28.3	996.150	$8.30.10^{-7}$	153.474
2014	29	995.947	$8.18.10^{-7}$	153.527
2015	27.8	996.292	$8.39.10^{-7}$	153.510
2016	28.2	996.178	$8.32.10^{-7}$	153.540
2017	27.5	996.377	$8.45.10^{-7}$	153.519
2018	28	996.236	$8.35.10^{-7}$	153.562

Calibration of the dynamometer was performed according to the ITTC procedure. Linear regression analysis was adopted as the standard uncertainty of the calibration. The accuracy of the dynamometer, estimated by the standard error estimation (*SEE*) of fitting to the calibration, can be one of the dominant sources of uncertainty in resistance measurement. The relative standard uncertainties corresponding to the calibration component were about 0.042% at *Fr* = 0.29 and 1.840% at *Fr* = 0.15, as shown in Figure 6. The uncertainty of the resistance measurements affected by temperature variation during the tests from 2010 to 2018 in fresh water at 27 °C to 29 °C was calculated. The corresponding component of uncertainty in the resistance measurement for each tow speed was about 0.122% at *Fr* = 0.29 and 0.216% at Fr = 0.15, as shown in Figure 7.

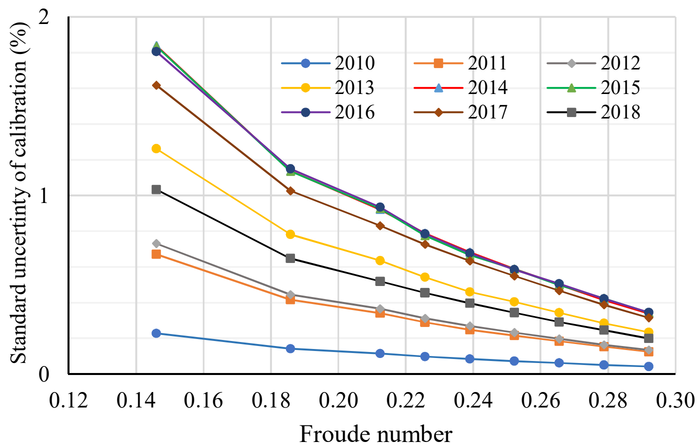

Figure 6 Standard uncertainty of calibration.

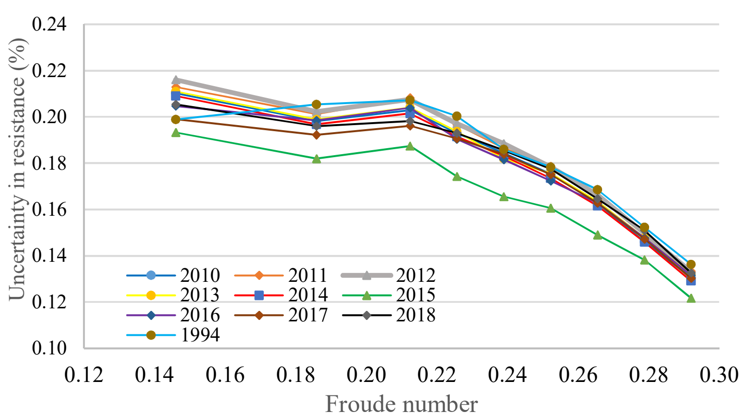

Figure 7 Uncertainty of resistance from temperature.

The standard uncertainty of any single test can be estimated by Eq. (7). A database of similar model tests can be quoted as an estimate. The standard deviations *(s)* from the measured resistance at *Fr* = 0.15 to 0.29 are shown in Table 5. It can be seen that the measurement uncertainty in the resistance tests for this hull model was about 0.506% at *Fr* = 0.15 and 0.962% at *Fr* = 0.29.

Table 4 Uncertainty of single resistance test runs.

Vm m/s	**Fr**	**R_T** kg	2010	2011	2012	2013	**s (%)** 2014	2015	2016	2017	2018
1.24	0.15	2.653	0.885	0.827	0.805	0.791	0.759	0.635	0.609	0.506	0.517
1.57	0.19	4.282	0.784	0.755	0.746	0.728	0.704	0.684	0.642	0.661	0.654
1.79	0.21	5.284	0.828	0.801	0.809	0.854	0.841	0.742	0.695	0.765	0.772
1.91	0.23	6.176	0.755	0.749	0.741	0.755	0.741	0.772	0.759	0.743	0.767
2.02	0.24	7.141	0.778	0.754	0.769	0.782	0.777	0.815	0.803	0.949	0.851
2.13	0.25	8.252	0.758	0.721	0.742	0.752	0.742	0.765	0.751	0.885	0.839
2.25	0.27	9.725	0.737	0.741	0.726	0.735	0.726	0.743	0.758	0.769	0.791
2.36	0.28	11.815	0.666	0.656	0.675	0.684	0.676	0.685	0.702	0.815	0.836
2.47	0.29	14.316	0.916	0.924	0.955	0.962	0.955	0.926	0.899	0.835	0.861

To obtain approximations of the true resistance value, the Kalman gains were tuned using an evolutionary algorithm to minimize the standard deviation from the sample resistance data. The results verified the effectiveness of the proposed approach for simultaneous estimation of the samples. The standard deviation value from the low-pass filter is compared with that from the Kalman filter in Figure 8. It is clear that the outcomes of the Kalman filter were more stable than those of the lowpass filter. The results show a significant improvement of the standard deviation, with a maximum of 0.082 kg for the KF and a maximum of 0.462 kg for the LPF at *Fr* = 0.15.

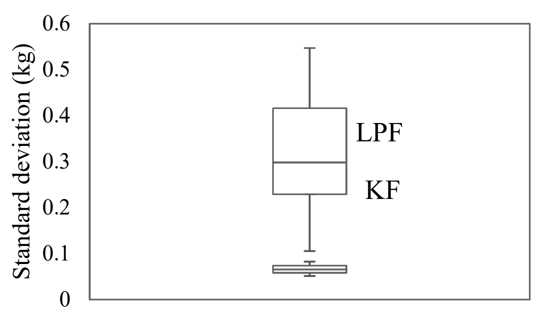

Figure 8 The standard deviation for the KF and the LPF.

The combination of uncertainty components related to the total resistance at *Fr* = 0.25 was multiplied through RSS (*Root-Sum-Square*), as summarized in Table 5.

The difference in standard deviation after filtering with the Kalman filter was reduced from 0.758 to 0.051 for 2010 and almost another year, indicating an overall improvement of over 90% in error reduction. The low standard deviation shows that the data were clustered closely around the mean (= more reliable). Therefore in the measurement of uncertainty, standard deviation is important: the lower the standard deviation, the less uncertainty and thus the higher the confidence in the experiment and thus the higher the reliability of the experiment. Reliable results can be obtained by optimization of the standard deviation with the application of a KF.

Table 5 Combined uncertainty (*fr* = 0.25) after filtering.

R_T (*Fr* = 0.25)	2010	2011	2012	2013	2014	2015	2016	2017	2018
Wetted area	0.126	0.126	0.126	0.126	0.126	0.126	0.126	0.126	0.126
Dynamometer	0.073	0.217	0.233	0.405	0.588	0.588	0.585	0.549	0.344
Temperature	0.175	0.179	0.166	0.166	0.173	0.166	0.166	0.175	0.166
Speed	0.066	0.066	0.066	0.066	0.066	0.066	0.066	0.066	0.066
Single test (deviation)	0.051	0.055	0.058	0.057	0.059	0.052	0.055	0.051	0.053
Combined	0.169	0.212	0.215	0.325	0.510	0.506	0.503	0.465	0.279

The measurement result and corresponding non-dimensional values (total resistance coefficient) are presented in Table 6. It can be seen that the measurement uncertainty in the resistance tests for this hull model was estimated at about 0.34% to 1.01% at *Fr* = 0.25. Coverage *k*p = 2 corresponds to a confidence level of 95% for a single test.

The accompanying statistical analysis quantifies values with mean differences from the single experimental test case between 2010 and 2018, which had a standard deviation of 0.06%. The present measurement uncertainties of towing tanks and their effects on the results can be further investigated using techniques for multiple time series analysis [24].

Table 6 Expanded uncertainty (*k*p = 2).

	2010	2011	2012	2013	2014	2015	2016	2017	2018
R_T (kg)	8.525 ±0.34%	8.278 ±0.42%	8.269 ±0.43%	8.267 ±0.65%	8.288 ±1.02%	8.438 ±1.00%	8.438 ±1.00%	8.227 ±0.93%	8.242 ±0.56%
C_T (10^{-3})	8.525 ±0.34%	3.890 ±0.42%	3.887 ±0.43%	3.897 ±1.02%	3.897 ±1.02%	3.915 ±1.01%	3.967 ±1.00%	3.867 ±0.93%	3.874 ±0.56%

4 Conclusions

A benchmark analysis of an experimental test of the LHI 007 Ro-Ro Ferry ship model was carried out from 2010 to 2018 based on the original 1994 data. The case study, with a range of speeds between 1.24 m/s and 2.47 m/s, demonstrated reasonable agreement.

The resistance test results were presented, including an uncertainty analysis to help improve the quality of the data and to identify potential problems in the results and possible improvements for future test techniques. The resistance data were observed using the KF and LPF schemes under the same conditions and their results were compared. The KF-based state estimation showed much better accuracy than the LPF-based state estimation in calculating the resistance, so the KF is suggested as the preferred choice. Further study, for example on the propulsion performance of similar hulls, is recommended.

Acknowledgment

The first author expresses his gratitude to the Ministry of Research, Technology and Higher Education (*Kemristekdikti*) for funding the research under a scheme known as the World Class Professor (WCP) program at ITS under contract number 2019/PKS/ITS/2018.

References

[1] Molland, A.F., Turnock, S.R. & Hudson, D.A., *Ship Resistance and Propulsion,* Cambridge, 2017.

[2] ISO, *Guide to the Expression of Uncertainty in Measurement*, International Organization for Standardization, Genève, Switzerland, 1995.

[3] Indonesian Hydrodynamic Laboratory (IHL), *Combined Performance Test in Towing Tank*, Report No. IHL 001-2-TT, 1994.

[4] Dang, J., Brouwer, J., Bosman, R. & Pouw, C., *Quasi-Steady Two-Quadrant Open Water Tests for the Wageningen Propeller C- and D-Series*, Proceedings of the 29th Symposium on Naval Hydrodynamics, 2012.

[5] Brouwer, J., Tukker, J. & Rijsbergen, M., *Uncertainty Analysis and Stationarity Test of Finite Length Time Series Signal*, The 4th International Conference Advanced Model Measurement Technologies for the Maritime Industry, 28-30 September, Istanbul Turkey, 2015.

[6] Steen S., Ankit & Gavrilin, S., *Uncertainty Analysis in Ship Model Resistance Test*, Proceeding of the ASME 2015 34th International Conference on Ocean, Offshore and Artic Engineering, 34, 2015.

[7] Brouwer J. & Klinkenberg Y.J.C., *Examining Random Uncertainty using A Newly Developed Power Spectrum Based Method*, Proceedings of the ASME 2016 35th International Conference on Ocean, Offshore and Arctic Engineering OMAE2016, Busan, Korea, 2016.

[8] Brunner C., Breitwieser C. & Muller Putz G.R., *SigViewer and Signal Server – Open-source Software Projects for bio Signal Analysis*, Biomed.

Eng./Biomed. Tech. **58**(SI-1-Track-TOC), 00001015152013, 2013. DOI: 1515/bmt-2013-toc-4194.

[9] Purnamasari, D., Dinariyana, A.A.B. & Purhadi, *Uncertainty Analysis on Resistance Test Model LCT 1000 DWT*, Master thesis, Institute of Technology Sepuluh Nopember (ITS), Surabaya, Indonesia, 2011. (Text in Indonesian)

[10] Purnamasari, D., Utama, I.K.A.P. & Suastika, I.K., *Comparative Resistance Test Between Two Towing Tanks (A Case Study at ITS and IHL),* Proceeding of the 14th International Conference on QIR (Quality in Research) ISSN 1411-1284, 2017. DOI:10.4028/www.scientific.net/AMM.874.114.

[11] Purnamasari, D., Utama, I.K.A.P. & Suastika, I.K., *Benchmark Study of Ship Model Resistance Test*, Applied Mechanics and Materials, , **874**, pp. 114-120, 2017.

[12] Ozdemir, Y.H., Barlas, B., Yilmaz, T. & Bayraktar, S., *Numerical and Experimental Study of Turbulent Free Surface Flow for a Fast Ship Model*, Journal of Brodogradnja/Shipbuilding, **65**(1), pp. 40-54, 2014.

[13] Samuel, Iqbal, M. & Utama, I.K.A.P., *An Investigation into the Resistance Components of Converting a Traditional Monohull Fishing Vessel into Catamaran Form*, International Journal of Technology, **6**(3), pp.432-441, 2015.

[14] Suastika, K., Nugraha, F. & Utama, I.K.A.P., *Parallel-Middle Body and Stern-Form Relative Significance in the Wake Formation of Single-screw Large Ships*, International Journal of Technology, **8**(1), pp. 92-101. 2017.

[15] Brouwer, J., Tukker, J. & Rijsbergen, M., *Uncertainty Analysis of Finite Length Measurement Signals*, The 3rd International Conference on Advanced Model Measurement Technology for the EU Maritime Industry (AMT'13), Gdansk, Poland, pp. 260-274. 2013.

[16] Durbin, J., Koopman, S.J., *Time Series Analysis by State Space Methods*. Oxford University Press, Oxford, 2nd edition, 2012.

[17] ITTC, *General Guidelines for Uncertainty Analysis in Resistance Test*, ITTC Procedure 7.5-02-02-02, 2014a.

[18] Coleman, H.W. & Steele W.G., *Experimentation and Uncertainty Analysis for Engineers.* John Wiley and Sons. Inc. New York, 1999.

[19] ITTC, *Practical Guide for Uncertainty Analysis of Resistance Measurement in Routine Tests,* Procedure 7.5-02-02-02.2, 2014c.

[20] Siqview v2.6 User Manual, 2012

[21] ITTC, *Density and Viscosity of Water*, ITTC Procedure 7.5-02-01-03, 2011.

[22] ITTC, *Uncertainty Analysis, Calibration Uncertainty*, ITTC Procedure 7.5-01-03-01, 2008.

[23] Menter, F.R., *Two-Equation Eddy-Viscosity Turbulence Models for Engineering Applications*, AIAA Journal, **32**(8), pp. 1598-1605, 1994.
[24] ITTC, *Report of Resistance Committee*, Proceedings of the 26th International Towing Tank Conference, Rio de Janeiro, Brazil, 2011.